![jove logo] **jove** Journal of Visualized Experiments   www.jove.com

Live Cell Imaging during Mechanical Stretch

Gabriel Rápalo[1,2], Josh D. Herwig[3], Robert Hewitt[4], Kristina R. Wilhelm[1,2], Christopher M. Waters[1,2], Esra Roan[3]

[1]Department of Physiology, University of Tennessee Health Science Center

[2]Department of Biomedical Engineering and Imaging, University of Tennessee Health Science Center

[3]Department of Biomedical Engineering, University of Memphis

[4]Department of Engineering Technology, University of Memphis

Correspondence to: Esra Roan at eroan@memphis.edu

Abstract

There is currently a significant interest in understanding how cells and tissues respond to mechanical stimuli, but current approaches are limited in their capability for measuring responses in real time in live cells or viable tissue. A protocol was developed with the use of a cell actuator to distend live cells grown on or tissues attached to an elastic substrate while imaging with confocal and atomic force microscopy (AFM). Preliminary studies show that tonic stretching of human bronchial epithelial cells caused a significant increase in the production of mitochondrial superoxide. Moreover, using this protocol, alveolar epithelial cells were stretched and imaged, which showed direct damage to the epithelial cells by overdistention simulating one form of lung injury *in vitro*. A protocol to conduct AFM nano-indentation on stretched cells is also provided.

Video Link

The video component of this article can be found at http://www.jove.com/video/52737/

Introduction

Cells are subjected to mechanical loads in many tissues, and this mechanical stimulation has been shown to promote changes in patterns of gene expression, release of growth factors, cytokines, or remodeling of the extracellular matrix and cytoskeleton[1-4]. The intracellular signals transduced from such mechanical stimuli occur through the process of mechanotransduction[5-7]. In the respiratory system, one outcome of mechanotransduction is the increase in reactive oxygen species (ROS)[8,9] and pro-inflammatory cytokines[10] in pulmonary epithelial cells in the presence of cyclic tensile strain. Strong evidence also suggests that excessive tensile strain leads to direct injury to the alveolar epithelium, in addition to the biochemical responses of cells[11-14]. Although the focus here is primarily on the response of lung cells to mechanical deformation, pathways induced by mechanotransduction play a key role in the basic function of many tissues in the human body, including the regulation of vascular tone[15] and the development of the growth plate[16].

The growing interest in mechanotransduction has resulted in the development of numerous devices for the application of physiologically relevant mechanical loads to cultured cells and tissue. In particular, devices applying a tensile strain, which is a common form of mechanical loading experienced by tissue, are popular [11,17-19]. However, many of the available devices are either designed as a bioreactor for tissue engineering applications or are not conducive to real time imaging with stretch. As such, there is a need to develop tools and methods that can visualize cells and tissues in tension to facilitate the investigation of pathways of mechanotransduction.

Herein, an in-plane mechanical stretching device was designed and protocols were developed to apply multiple forms of strain to tissues and cells while allowing imaging of the biochemical and mechanical responses in real time (**Figure 1A-D**). The device utilizes six evenly spaced clamps arranged circumferentially to grasp a flexible membrane and apply an in-plane, radial distention up to approximately 20% (**Figure 1B**). The actuating device can be placed in a cell culture incubator for an extended period of time, while the motor (**Figure 1C**) is positioned outside the incubator and controlled by proprietary software provided by the motor supplier. The motor is connected to a linear driver, which rotates an internal cam, driving the six stretcher clamps uniformly in tension and relaxation.

In addition to the mechanical device, customized flexible membranes were created from commercially available cell culture ready membranes to be used in the mechanical system. Then circular walls (with a diameter of approximately 28 mm) were made and attached on to the flexible membrane so that cells could be cultured only in this region of well-described strain profile. In order to determine whether the placement of these membranes within the actuating device would provide uniform and isotropic strain in the center of the flexible membrane, finite element analysis was conducted using commercially available software (**Figure 1E-F**). The flexible membrane was modeled with symmetric boundary conditions and utilizing all quadrilateral elements for the mesh. The concentric rings seen in the contour plot of maximum principal strain shown in **Figure 1F** indicate the isotropic distribution of the strain.

The strain experienced by the membrane was measured by recording images of markings through loading (**Figure 2**). **Figure 2D** shows that the average membrane strain measured in radial and axial directions was approximately linear with respect to the applied motor counts up to a maximum linear strain of 20%. There was no significant difference between the strain levels measured during distention compared with those measured during retraction back to the resting position. Next, the displacement of human bronchial epithelial cells (16HBE) and their nuclei cultured on the custom flexible membrane were measured. Fluorescently labeled (DAPI) nuclei of the 16HBE cells were imaged using a 20X objective under a confocal microscope, whereas whole cell displacement was measured with phase contrast images recorded with a digital microscope. As seen in **Figure 3**, the strain measured by displacement of nuclei was similar to that measured by displacement of markings on the membrane, up to ~20% linear strain. This confirms that the strain applied to the membranes was transmitted to the adherent cells. The protocols describing the use of the custom device on a traditional microscope and an atomic force microscope are provided in the following steps.

Protocol

1. Construction of Membrane with Well Walls for Retention of Cell Culture Media (see Figure 1D for the final product)

1. Using polydimethylsiloxane (PDMS) sheets coated with Collagen I, cut the outline of the flexible membrane with a scalpel or a die.
2. Place each membrane in a 60 mm Petri dish for storage.
3. Creation of walls:
    1. Mix PDMS at a 10:1 weight ratio of elastomer A to elastomer B (curing agent).
    2. Pour 5 ml of fully mixed PDMS into 50 ml tubes.
    3. Place 50 ml tubes with uncured PDMS horizontally in a hybridization oven.
    4. Use the rotor function to coat the inner walls of the tubes at 8 rpm during the curing time. At RT, the PDMS will be fully cured in 2 days.
    5. Remove the PDMS from the tube in a sterile cell culture hood.
    6. Using a new razor blade, partition the cylinder of PDMS into sections 4 mm in height.
    7. Place the sections, which will serve as the membrane walls, into a Petri dish container without allowing the walls to become creased.
4. Select and center one wall of PDMS on one membrane while maintaining the two in the Petri dish.
5. Gently place uncured PDMS (10:1 ratio) on the outside perimeter of the wall to be used as glue. Prevent formation of gaps between the wall and the membrane since it is there to retain liquid.
6. Place each Petri dish containing the completed membrane and covered in an oven at 70 °C for 24 hr to cure.

2. Correlation of Motor Rotations with Clamp Displacement or Radial Growth for Calibration (Figure 2)

1. Start the software controlling the motor.
2. Displace the clamps of the device using the manual setting in the motor software.
3. Measure the distance and record the motor count position between opposing clamps at both minimum and maximum displacement of the clamps.
4. Calculate the percent change in the distance between the clamps as a function of the motor count (~0-75k counts). This will indicate the maximum potential strain achieved on the membrane.

3. Application of Stretch on Mouse Lung Epithelial Cell Line (MLE12)

1. Seed MLE12 cells at 2.5 million cells on the flexible membrane (Step 1) per well to be confluent within two days. The seeding density may vary for different cell types.
2. Make sure the mechanical actuator is in a fully relaxed position.
    1. Remove cell culture media.
    2. Using 1.5 mm biopsy punches, punch two holes in each of the six clamp (see **Figure 1D**) tabs of the membrane. The radial placement of the holes determines the amount of pre-tension the membrane experiences initially. Punch the holes at a radius of 20.5 mm on the membrane tabs if no pre-tension is desired.
    3. Position the membrane on the stretcher with the punched holes lining up with the pins within the clamps. Place top clamps in place. Tighten the screws one at a time alternating sides.
    4. Add 1 ml cell culture media.
3. Place the device on the microscope stage centering the middle of the membrane with the light path.
4. Use tape or magnets (if possible) to fix the device to the stage. Once fixed, control the in-plane (parallel to the membrane) and vertical (z-direction) of the mechanical device with the stage controller of the microscope.
5. Apply stretch with the software provided by the manufacturer by manually controlling the position and speed of motor rotation[20].

4. Measurement of Mitochondrial Reactive Oxygen Species (ROS)

1. Once cells are confluent, add 1-2 ml of RT DMEM with mitochondrial superoxide indicator (5 µM final concentration) directly on the cells.
2. Incubate for 10 min at 37 °C.
3. Wash cells gently three times with buffer warmed in a water bath to 37 °C.
4. Immediately place the flexible membrane on the stretcher (Step 2.2) already in place under an upright confocal microscope.

5. Add 1 ml of DMEM with phenol-red free medium and 25 mM of HEPES.
6. Set excitation/emission filters to 510/580 nm.
7. Image multiple fields every 15 min to create the desired time course of mitochondrial superoxide production.
8. From captured images, record fluorescence intensity histograms at each time interval using software capable of quantifying fluorescence intensity.

5. Application of Stretch and Atomic Force Microscopy (AFM)

NOTE: These steps are provided for a specific AFM and optical microscope combination (**Figure 4** and Materials List).

1. Prepare the AFM for the experiment.
    1. Increase the height of the AFM head to its maximum position in the z-direction.
    2. Put extenders on the legs of the AFM to lift the plane at which AFM cantilever contacts the sample. The specimen and the AFM head needs to be lifted to accommodate the height of the mechanical device.

2. Prepare the optical microscope (if available).
    1. Remove the AFM scanner plate. Remove the desired objective.
    2. Add a spacer to the objective. The height of the spacer would depend on the objective and the specific AFM set-up, but it is necessary if optical imaging is desired since observation plane will be shift in the z-direction by an amount equal to the stretcher and adapter height (**Figure 5A**). Note that the AFM usually provides low magnification imaging from an optical path above the device.
    3. Mount the desired objective back in its location. Place the scanner back on to the AFM.
    4. Start the AFM software. Start all necessary light sources including the light source for fluorescence measurements.
    5. Mount a chip with a cantilever beam that is appropriate for the desired measurements. 200 pN/nm or less stiffness is preferred when measuring the elastic modulus of live cells.
    6. Align the laser and calibrate the cantilever stiffness according to manufacturer's suggestions on a glass coverslip mounted on the device.

3. Prepare a membrane as in Step 1, but with the following modifications.
    1. Immediately before mounting the membrane on to the stretching device, cut the walls to about 1 mm in height. This prevents the interference experienced between the membrane walls and the load cell.
    2. Mount the membrane on the mechanical device as described 3.2.1-3.2.3.
    3. Remove cell culture media to prevent damage to the AFM scanner in case of a spill.
    4. Couple the device with an adapter (**Figure 5A**). Place the mechanical device with the adapter on the scanner.
    5. Stretch the membrane to the desired tensile strain level.

4. Nano-indentation of stretched cells.
    1. Add a limited (<0.5 ml) volume of media on the cells to avoid AFM scanner or microscope damage due to a spill.
    2. Engage the cantilever beam with the membrane.
    3. Follow the protocol of the particular AFM device to scan areas of interest.

Representative Results

Reactive Oxygen Species and Deformation

Previous studies have shown increases in reactive oxygen species (ROS) in airway and alveolar epithelial cells in response to cyclic stretch[21]. Reactive oxygen species include molecules and free radicals derived from molecular oxygen with high reactivity to lipids, proteins, polysaccharides, and nucleic acids[22-24]. ROS serve as a common intracellular signal to regulate ion channel function, protein kinase/phosphatase activation, and gene expression, but excessive or unregulated production can contribute to apoptotic and necrotic cell death, neurodegeneration, atherosclerosis, diabetes, and cancer[24,25]. Superoxide, a pre-cursor for other forms of ROS, can be produced as a by-product of mitochondrial respiration when electrons leak from the electron transfer chain. Previous studies suggested that cyclic mechanical stretch stimulated the production of superoxide through a combination of the NADPH oxidase system (nicotinamide adenine dinucleotide phosphate-oxidase) and the mitochondrial electron transport chain (complex I and III). It has been proposed that this stimulation was due to a direct distortion of the mitochondria[21] possibly due to connections to the cell cytoskeleton. In order to test this hypothesis, the cell stretching device was developed so that we could image changes in ROS production in live cells in response to mechanical stretch. Here, the mitochondrial ROS produced by bronchial epithelial cells due to stretch was measured using the custom device and protocol. In the absence of mechanical stretch, ROS production did not significantly increase over 60 min (**Figure 4**). When a single 17% stretch was applied and maintained, there was an increase in mitochondrial ROS that persisted for another 60 min.

Direct Epithelial Monolayer Damage Due to Stretch

Indirect mechanisms by which excessive stretch in the lung epithelium harms the lungs have been discussed in depth elsewhere[2]. Several studies suggest that excessive mechanical stretch of lung epithelial cells can cause direct injury involving damage to cells[11,13,26,27]. This type of damage is difficult to capture without real-time imaging during the mechanical distention. As such, utilizing the custom device and phase contrast microscopy consecutive images of cells that were mechanically stretched were recorded before and after treatment with a pro-inflammatory cytokine (50 ng/ml TNF-α for 6 hr) (**Figure 5**). Images of the same field of cells were captured at increasing strain levels. The images show the formation of a gap when the cells were stretched between 10 and 15% strain as indicated by the red arrows. It is important to note that these images were recorded in near real-time, <10 sec of lag between the end of stretch and imaging, while the cells were stretched. In previous

studies of cell imaging of stretched cells, images were obtained before and after stretch comparing only the images of cells not at stretched condition[11,13,28].

AFM Nano-indentation on stretched cells

The mechanical device was placed in the AFM with the use of an adapter plate (see **Figure 6A**). Using previously published methods[13], elastic modulus maps (E-maps) of MLE12 cells before and after 10% tensile strain were obtained (**Figure 6D-E**). Although phase contrast image at 10% strain (**Figure 6D**) was obtained within 10 sec of the stretch, the E-maps shown in **Figure 6D-E** consumed approximately 22 min with 300 individual force-deflection curves recorded over a 40 μm X 40 μm area with a 2.5 μm/s velocity of the tip in the z-direction. Please click here to view a larger version of this figure.
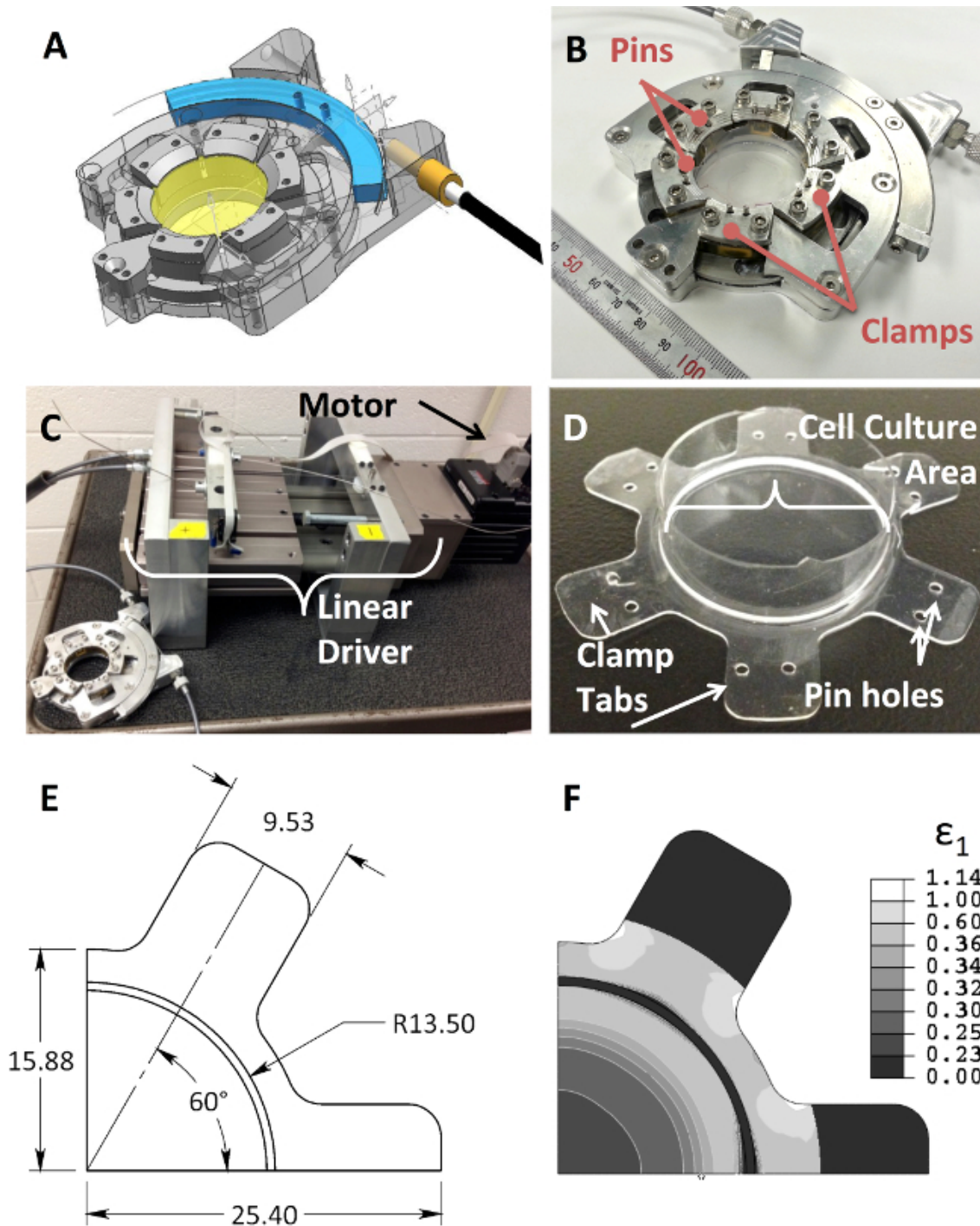
Figure 1. The custom designed device for cell culture and stretching. (**A**) Computer-generated drawing of the mechanical design of the device, (**B**) photograph of the completed device, (**C**) photograph of device connected to the motor and linear driver, which converts the motor rotation into a 1-dimensional motion which controls the clamp biaxial stretch of the (**D**) silicone rubber membrane. The substrate contains two holes on each clamp tab to be placed on posts on each clamp. (**E**) Dimensioned FEA model of the flexible membrane that is $1/4$ of the whole structure due to use of symmetric boundary conditions. (**F**) Maximum principal strain is shown in the full membrane depicting the formation of rings indicative of isotropic strain field. Please click here to view a larger version of this figure.

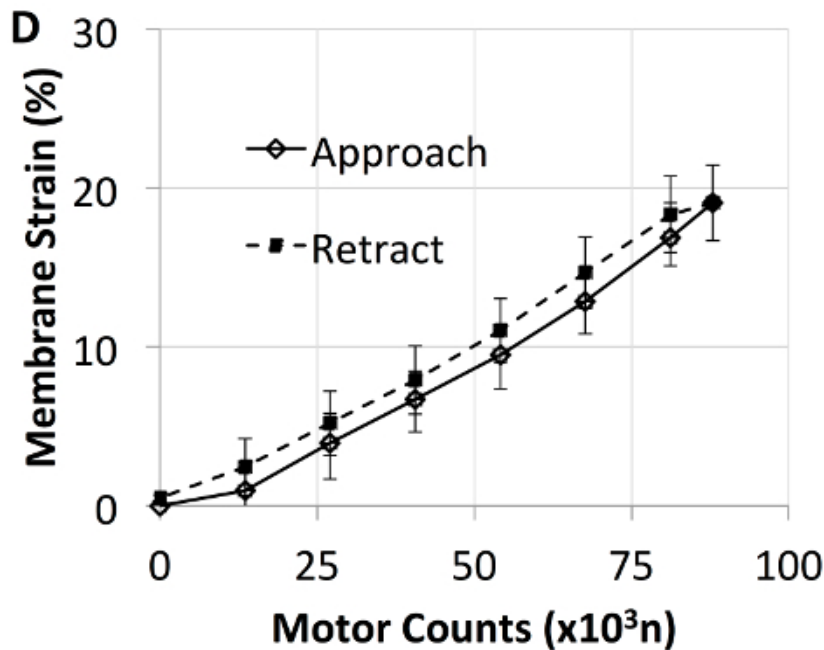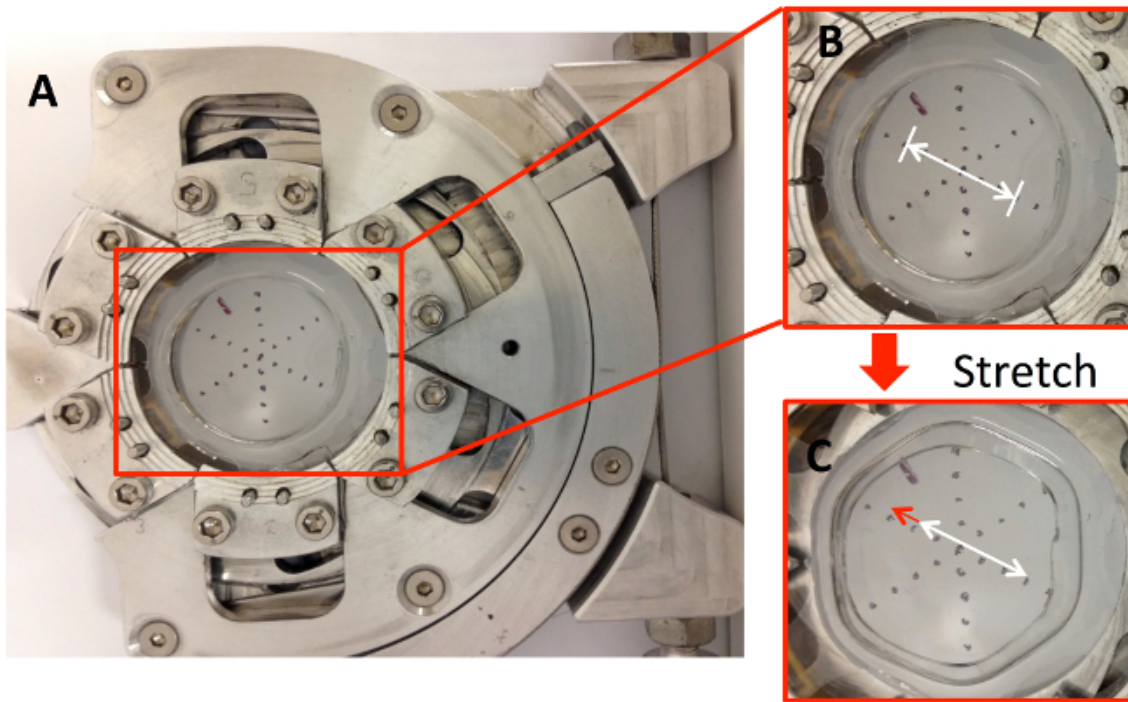**Figure 2.** (**A**) The device supporting a flexible membrane with markings applied to measure applied strain is shown. Close-up images of the markings, before (**B**) and after (**C**) stretch, were labeled with an arrow to clearly indicate the displacement of the markings on the membrane. (**D**) Membrane strain as a function of the motor counts during approach and retraction. Membrane strain was similar in both approach and retraction with retraction producing slightly higher strains. Please click here to view a larger version of this figure.

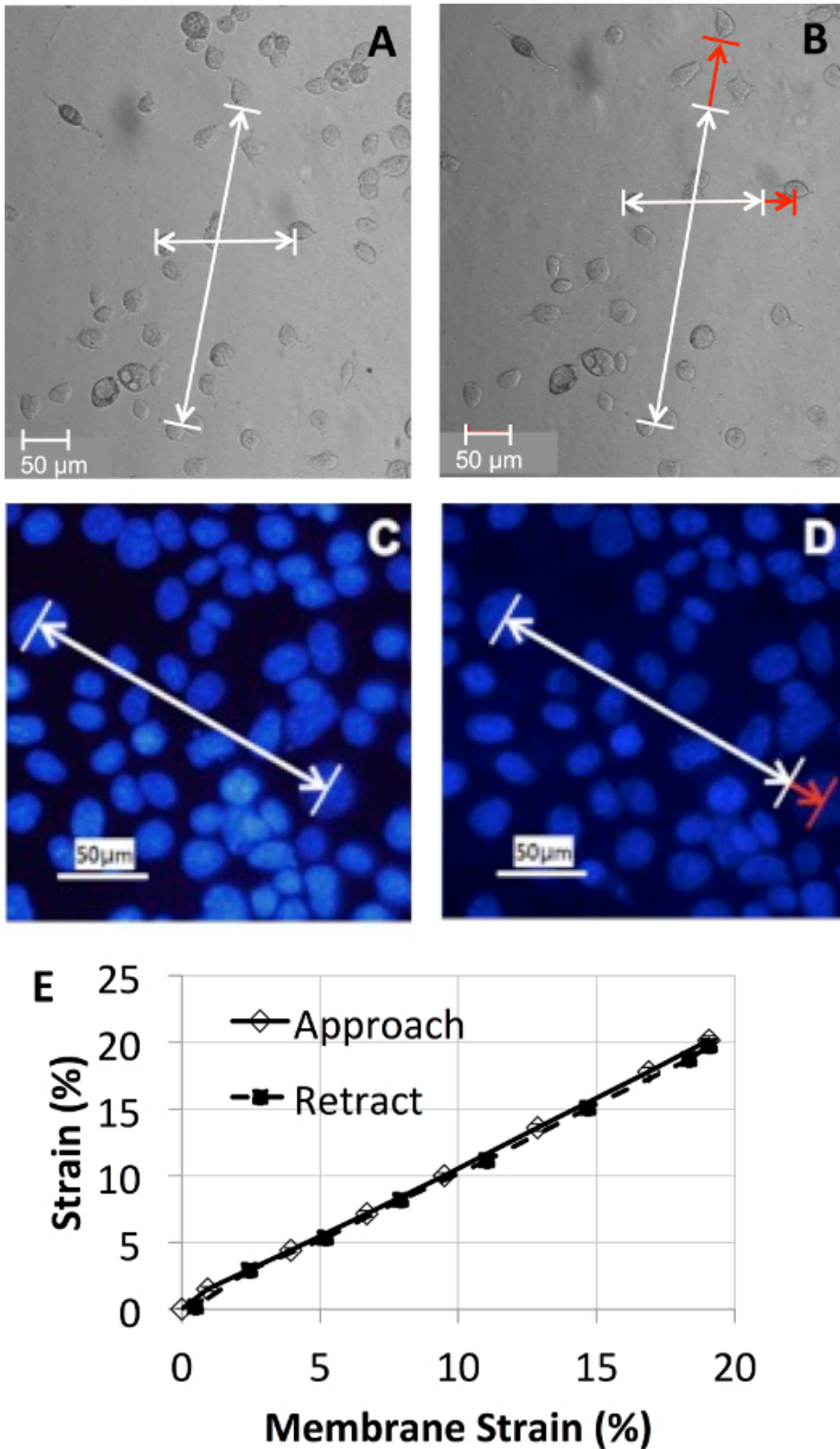**Figure 3. Membrane strain transmission to the cells.** (**A**-**B**) Phase contrast images of human bronchial epithelial cells (16HBE) on the flexible membrane using a 10X objective, before (**A**) and after (**B**) 20% strain. (**C**-**D**) Fluorescently labeled (DAPI) nuclei of the 16HBE cells were imaged using a 20X objective under a confocal microscope, before (**C**) and after (**D**) 20% strain. (**E**) The membrane strain experienced by cells was linear and homogenous. Please click here to view a larger version of this figure.
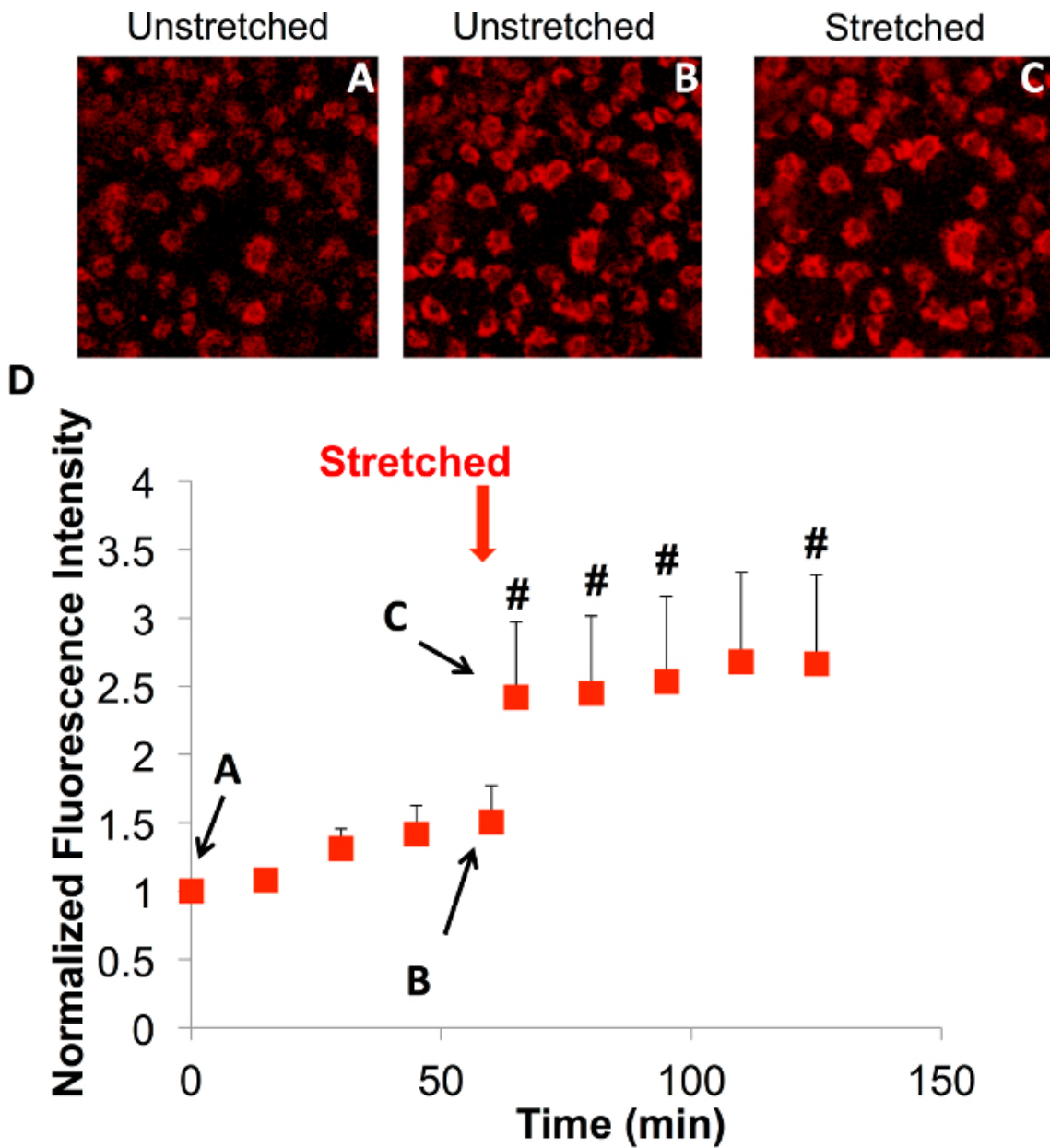
Figure 4. The impact of a single stretch on the ROS production of 16HBE cells was observed using a cumulative mitochondrial superoxide sensor using a 20X objective under a confocal microscope. (A-C) Snapshots of the time course (0, 60 min, and ~65 min) of superoxide production during stretch in the same field of cells. (D) Relative fluorescence intensity of 16HBE cells over time indicating a 50% increase in fluorescence intensity from baseline production of superoxide within the first hour (A to B). Please click here to view a larger version of this figure.
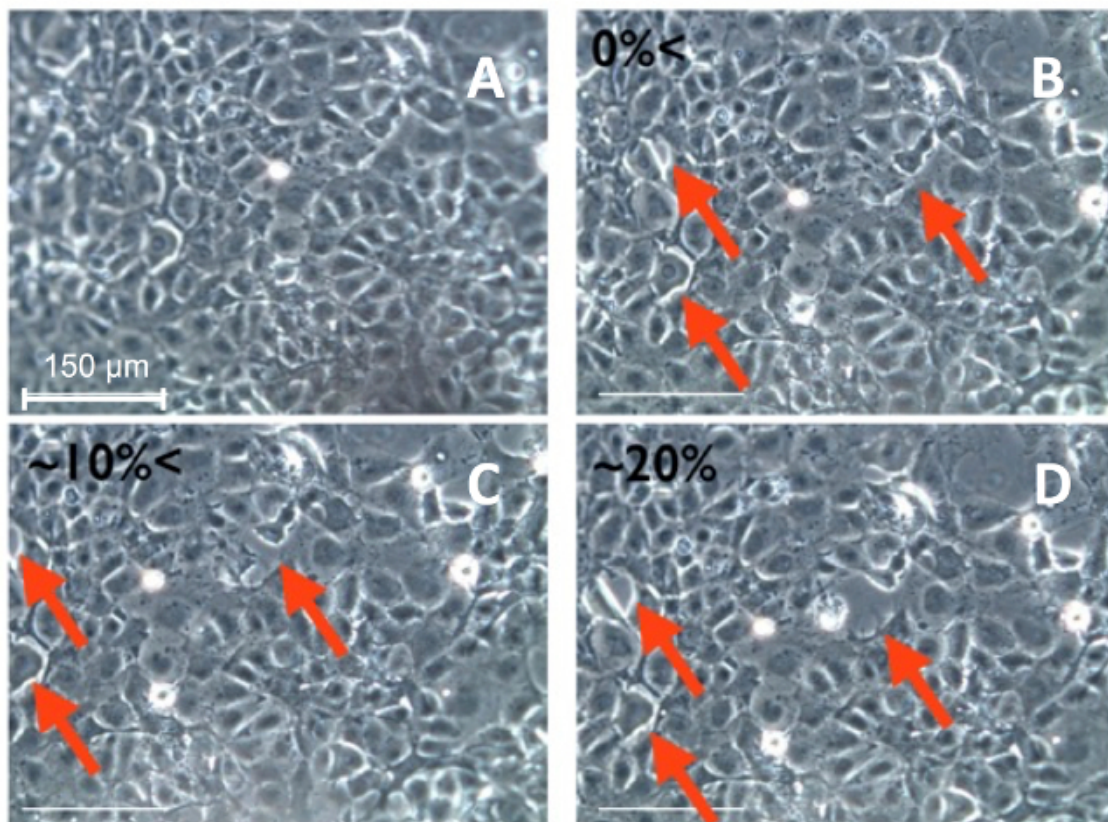
Figure 5. Phase contrast images of an alveolar epithelial (MLE12) monolayer response to increasing stretch. (**A**-**D**) were all recorded using a digital microscope with a 20X objective. The arrows indicate the locations where cell-to-cell separation occurred. Please click here to view a larger version of this figure.
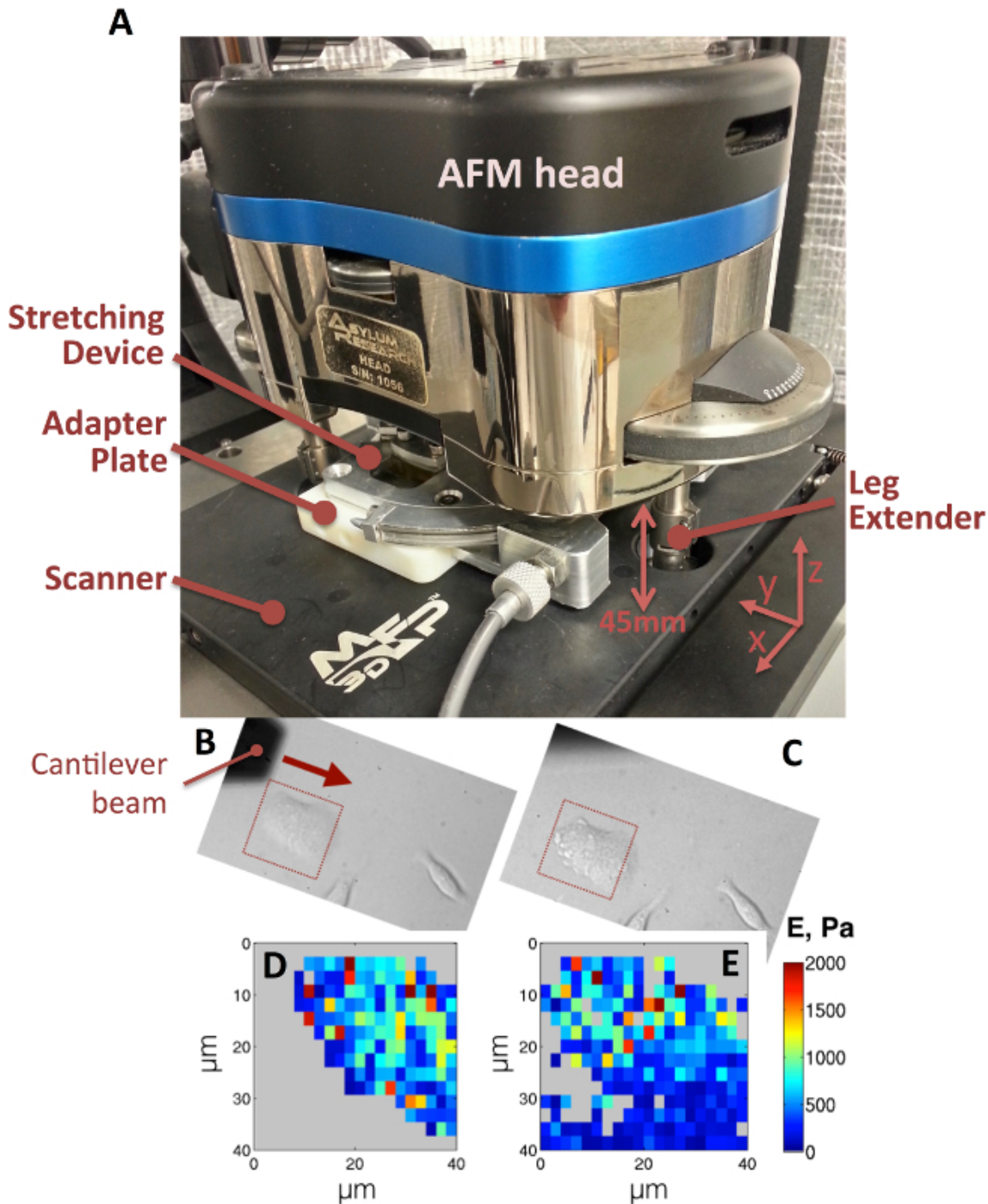
Figure 6. (A) Mechanical device shown in the AFM for nano-indentation of cells with stretch. The scanner must be removed for the placement of objective extender. Three leg extenders are attached to all three legs of the AFM head to allow for device placement. An adapter plate is utilized to mount the stretcher on to the AFM scanner (black plate). The cantilever beam scans in the direction of the arrow shown in the before stretch phase contrast image an MLE12 cell (**B**). The red squares in the before (**B**) and after (**C**) stretch images depict the area that was captured during nano-indentation (40X objective). The elastic modulus maps, before (**D**) and after (**E**) stretch, are obtained with previously published analysis techniques[13]. Please click here to view a larger version of this figure.

Discussion

A unique device for live cell imaging during mechanical stretch was developed; and this device was used in a protocol to study lung epithelial cell mechanobiology. In preliminary studies, it was found that a single held stretch stimulated the production of mitochondrial superoxide in bronchial epithelial cells. In addition, it was demonstrated that increased levels of mechanical strain caused direct damage to the integrity of a monolayer of alveolar epithelial cells.

To conduct these preliminary experiments, the device was first calibrated, and then it was shown that the membrane strain was transmitted to cells (**Figures 2-3**). Overall the device performed well, as indicated by the close correlation between the membrane strain (measured by marks on the membrane) and the cell strain (measured by distances between nuclei) shown in **Figure 3E**. However, there were some minor differences observed between strain measured on the membranes during the approach and the return curves of the markers, as shown in **Figure 2D**. This was likely due to backlash in the device and possibly related to gripping issues. In addition, a universal mounting mechanism for the device is needed so that it can efficiently be used on microscopes with different configurations. This would reduce the time spent between positioning of the device and image acquisition while maintaining a robust connection to the microscope. Holes punched in the membranes were used to apply a minor pre-strain to the membrane to prevent formation of an initial compressive state due to clamping of an elastic material. The compressive state also leads to a reduction of maximum applicable strain.

The custom device was designed to fit in an Asylum MFP3D Atomic Force Microscope to allow nano-indentation of live cells during mechanical stretch. We are not aware of any other device that is capable of inducing an isotropic stress state in the imaging plane that can function within an AFM. The device was also designed for continuous use in a cell-culture incubator (kept at 37 °C in a humid, sterile environment with 5% CO_2). The ability to function within an incubator allows the study of cells undergoing long-term stretch regimens.

There are several limitations to the presented approach. First, as the membrane stretches, the field of focus moves out of plane, although minimally (~100 µm). This becomes a limitation when tracking a field of cells through a stretch regimen, because the field of view changes over the course of the membrane distention. Even though membrane within the 22 mm diameter experiences 0.23-0.25 strain, the regions outside of this inner diameter experience a more variable strain field. Although imaging studies are easily limited to this central region, it is possible that the cells responding to higher levels of strain at outer regions can impact the response of cells within the central region. A uniform strain distribution over a larger area of interest can be achieved with improvements in the membrane design. The PDMS membrane is auto-fluorescent at wavelengths commonly used for fluorescent indicators, and this limits the capability for imaging fluorescence in cells from beneath the membrane. For this reason an upright microscope was utilized with water immersion objectives in our studies of ROS production described above. This can be a limitation for studies in which AFM and fluorescence imaging are combined.

The most common commercial device (FlexCell FX 5000 Tension System) for applying mechanical strain to cells incorporates a controllable vacuum system applying tensile strain on a membrane while moving in and out of the optical plane. The membrane and clamp design presented herein create a bi-axial strain field where strain is isotropic and remains in plane allowing real-time imaging. With minor modifications to the membrane design, the stretcher can produce uniaxial stretch modes as well. If the cells are first seeded on a distended membrane, in-plane compressive loads can also be applied. The device is able to reach both physiological and pathological levels of strain. In summary, a new device and protocols were developed that can be used to apply mechanical strain to live cells that can be imaged using fluorescence microscopy and AFM nano-indentation.

Disclosures

The authors declare that they have no competing financial interests.

Acknowledgements

References

1. Tschumperlin, D. J., Boudreault, F.,, & Liu, F. Recent advances and new opportunities in lung mechanobiology. *J Biomech.* **43**, 99-107, doi: 10.1016/j.jbiomech.2009.09.015 (2010).
2. Waters, C. M., Roan, E., & Navajas, D. in *Comprehensive Physiology.* John Wiley, & Sons, Inc., (2011).
3. Majkut, S., Dingal, P. C. D. P., & Discher, D. E. Stress Sensitivity and Mechanotransduction during Heart Development. *Current Biology.* **24**, R495-R501, doi: 10.1016/j.cub.2014.04.027 (2014).
4. Hoffman, B. D., Grashoff, C., & Schwartz, M. A. Dynamic molecular processes mediate cellular mechanotransduction. *Nature.* **475**, 316-323, doi: 10.1038/nature10316 (2011).
5. Wang, N., Butler, J. P., & Ingber, D. E. Mechanotransduction across the cell-surface and through the cytoskeleton. *Science.* **260**, 1124-1127, doi: 10.1126/science.7684161 (1993).
6. Liu, M., Tanswell, A. K., & Post, M. Mechanical force-induced signal transduction in lung cells. *Am J Physiol.* **277**, L667-683 (1999).
7. Janmey, P. A., & McCulloch, C. A. Cell mechanics: integrating cell responses to mechanical stimuli. *Annu Rev Biomed Eng.* **9**, 1-34, doi: 10.1146/annurev.bioeng.9.060906.151927 (2007).
8. Waters, C. M. Reactive oxygen species in mechanotransduction. *Am J Physiol Lung Cell Mol Physiol.* **287**, L484-485, doi: 10.1152/ajplung.00161.2004 (2004).
9. Chapman, K. E. *et al.* Cyclic mechanical strain increases reactive oxygen species production in pulmonary epithelial cells. *Am J Physiol Lung Cell Mol Physiol.* **289**, L834-841, doi: 10.1152/ajplung.00069.2005 (2005).
10. Chu, E. K., Whitehead, T., & Slutsky, A. S. Effects of cyclic opening and closing at low- and high-volume ventilation on bronchoalveolar lavage cytokines. *Crit Car Med.* **32**, 168-174, doi: 10.1097/01.ccm.0000104203.20830.ae (2004).

11. Tschumperlin, D., & Margulies, S. Equibiaxial deformation-induced injury of alveolar epithelial cells *in vitro*. *Am J Physiol.* **275**, L1173-1183 (1998).
12. Vlahakis, N. E., & Hubmayr, R. D. Cellular stress failure in ventilator-injured lungs. *Am J Respir Crit Care Med.* **171**, 1328-1342, doi: 10.1164/rccm.200408-1036SO (2005).
13. Roan, E. *et al.*Hyperoxia alters the mechanical properties of alveolar epithelial cells. A*m J Physiol Lung Cell Mol Physiol* 302, L1235-1241, doi: 10.1152/ajplung.00223.2011 (2012).
14. Gamerdinger, K. *et al.* Mechanical load and mechanical integrity of lung cells - Experimental mechanostimulation of epithelial cell- and fibroblast-monolayers. *J Mech Behav Biomed Mater 4 0*, 201-209, doi: 10.1016/j.jmbbm.2014.08.013 (2014).
15. Hayashi, K., & Naiki, T. Adaptation and remodeling of vascular wall; biomechanical response to hypertension. *J Mech Behav Biomed Mater.* **2**, 3-19, doi: 10.1016/j.jmbbm.2008.05.002 (2009).
16. Villemure, I., & Stokes, I. Growth plate mechanics and mechanobiology. A survey of present understanding. *J Biomech.* **42**, 1793-1803, doi: 10.1016/j.jbiomech.2009.05.021 (2009).
17. Waters, C. M. *et al.* A system to impose prescribed homogenous strains on cultured cells. *J Appl Physiol (1985).* **91***,* 1600-1610 (2001).
18. Gerstmair, A., Fois, G., Innerbichler, S., Dietl, P., & Felder, E. A device for simultaneous live cell imaging during uni-axial mechanical strain or compression. *J Appl Physiol (1985).* **107**, 613-620, doi: 10.1152/japplphysiol.00012.2009 (2009).
19. Dassow, C. *et al.* A method to measure mechanical properties of pulmonary epithelial cell layers. *J. Biomed. Mater. Res. Part B Appl. Biomater.* **101**, 1164-1171, doi: 10.1002/jbm.b.32926 (2013).
20. Animatics Corporation, *SmartMotor User's Guide v523.* http://www.animatics.com/download/publication/UsersGuide%20v523.pdf (2011).
21. Chapman, K. *et al.* Cyclic mechanical strain increases reactive oxygen species production in pulmonary epithelial cells. *Am J Physiol Lung Cell Mol Physiol.* **289**, L834-841, doi: 10.1152/ajplung.00069.2005 (2005).
22. Birukov, K. G. Cyclic stretch, reactive oxygen species, and vascular remodeling. *Antioxid Redox Signal.* **11***,* 1651-1667, doi: 10.1089/ARS.2008.2390 (2009).
23. Turrens, J. F. Mitochondrial formation of reactive oxygen species. *J Physiol.* **552***,* 335-344, doi: 10.1113/jphysiol.2003.049478 (2003).
24. Wang, W. et a*l. Supe*roxide flashes in single mitochondria. *Cell.* **134***,* 279-290, doi: 10.1016/j.cell.2008.06.017 (2008).
25. Pouvreau, S. Superoxide flashes in mouse skeletal muscle are produced by discrete arrays of active mitochondria operating coherently. *PLoS One.* **5***,* doi: 10.1371/journal.pone.0013035 (2010).
26. Yalcin, H. C. et a*l. Infl*uence of cytoskeletal structure and mechanics on epithelial cell injury during cyclic airway reopening. *Am J Physiol Lung Cell Mol Physiol.* **297**, L881-891, doi: 10.1152/ajplung.90562.2008 (2009).
27. Jacob, A. M., & Gaver, D. P. Atelectrauma disrupts pulmonary epithelial barrier integrity and alters the distribution of tight junction proteins ZO-1 and claudin 4. *J Appl Physiol.* **113***,* 1377-1387, doi: 10.1152/japplphysiol.01432.2011 (2012).
28. DiPaolo, B. C., Lenormand, G., Fredberg, J. J., & Margulies, S. S. Stretch magnitude and frequency-dependent actin cytoskeleton remodeling in alveolar epithelia. *Am J Physiol Cell Physiol.* **299***,* C345-353, doi: 10.1152/ajpcell.00379.2009 (2010).